8-1-2013

In vivo Imaging of Human Retinal Microvasculature Using Adaptive Optics Scanning Light Ophthalmoscope Fluorescein Angiography

Alexander Pinhas
New York Icahn School of Medicine at Mount Sinai

Michael Dubow
New York Icahn School of Medicine at Mount Sinai

Nishit Shah
New York Eye and Ear Infirmary

Toco Y.P. Chui
New York Eye and Ear Infirmary

Drew Scoles
University of Rochester

See next page for additional authors

Accepted version. *Biomedical Optics Express*, Vol. 4, No. 8 (August 2013): 1305-1317. DOI.

In vivo imaging of human retinal microvasculature using adaptive optics scanning light ophthalmoscope fluorescein angiography

Alexander Pinhas[1,2,10]
Department of Ophthalmology, New York Eye & Ear Infirmary
Icahn School of Medicine at Mount Sinai
New York, NY
Michael Dubow[1,2,10]
Department of Ophthalmology, New York Eye & Ear Infirmary
Icahn School of Medicine at Mount Sinai
New York, NY
Nishit Shah[1]
Department of Ophthalmology, New York Eye & Ear Infirmary
New York, NY
Toco Y. Chui[1]
Department of Ophthalmology, New York Eye & Ear Infirmary
New York, NY
Drew Scoles[3]
3Department of Biomedical Engineering, University of Rochester
Rochester, NY

Biomedical Optics Express, Vol. 4, No. 8 (August 2013): pg. 1305-1317. DOI.

Yusufu N. Sulai[4]
The Institute of Optics, University of Rochester
Rochester, NY
Rishard Weitz[1]
Department of Ophthalmology, New York Eye & Ear Infirmary
New York, NY
Joseph B. Walsh[1]
Department of Ophthalmology, New York Eye & Ear Infirmary
New York, NY
Joseph Carroll[5,6,7,8]
Department of Ophthalmology, Medical College of Wisconsin
Department of Biomedical Engineering, Marquette University
Department of Biophysics, Medical College of Wisconsin
Department of Cell Biology, Neurobiology & Anatomy, Medical College of Wisconsin
Milwaukee, WI
Alfredo Dubra,5,6,7
Department of Ophthalmology, Medical College of Wisconsin
Department of Biomedical Engineering, Marquette University
Department of Biophysics, Medical College of Wisconsin
Milwaukee, WI
Richard B. Rosen[1,9,*]
Department of Ophthalmology, New York Eye & Ear Infirmary
New York, NY
Department of Ophthalmology, New York Medical College
Valhalla, NY

Abstract: The adaptive optics scanning light ophthalmoscope (AOSLO) allows visualization of microscopic structures of the human retina *in vivo*. In this work, we demonstrate its application in combination with oral and intravenous (IV) fluorescein angiography (FA) to the *in vivo* visualization of the human retinal microvasculature. Ten healthy subjects ages 20 to 38 years were

Biomedical Optics Express, Vol. 4, No. 8 (August 2013): pg. 1305-1317. DOI.

imaged using oral (7 and/or 20 mg/kg) and/or IV (500 mg) fluorescein. In agreement with current literature, there were no adverse effects among the patients receiving oral fluorescein while one patient receiving IV fluorescein experienced some nausea and heaving. We determined that all retinal capillary beds can be imaged using clinically accepted fluorescein dosages and safe light levels according to the ANSI Z136.1-2000 maximum permissible exposure. As expected, the 20 mg/kg oral dose showed higher image intensity for a longer period of time than did the 7 mg/kg oral and the 500 mg IV doses. The increased resolution of AOSLO FA, compared to conventional FA, offers great opportunity for studying physiological and pathological vascular processes.

1 - Introduction

Fluorescein angiography (FA) is the standard clinical tool for assessing retinal and choroidal vascular disease. Since its introduction in 1961 by Novotny and Alvis [1], its use has continued to grow, with more than 1.2 million public procedures reported in 2011 by Medicare [2]. FA reveals important pathological features of common vascular conditions including microaneurysms, vascular leakage, capillary non-perfusion and neovascularization. In a variety of less common diseases, such as sickle cell retinopathy, hereditary macular diseases and retinal tumors, clinicians rely on FA to reveal characteristic patterns which help facilitate diagnosis and monitor treatment response [3].

Despite its ubiquity in the modern eye care practice, intravenous (IV) FA is an invasive procedure and is associated with infrequent but potentially severe adverse reactions, and even rare anaphylactoid responses and death [4–8]. In order to acquire the early filling sequence, the photographer must image the eye within seconds following dye injection to capture its first appearance in the retinal vasculature. For diseases where early filling information is not critical, several investigators have demonstrated that oral administration of fluorescein allows a more extended imaging period [9–14]. Conditions as diverse as diabetic retinopathy, cystoid macular edema, central serous retinopathy and papilledema have been successfully imaged using oral fluorescein with comparable quality to IV fluorescein [9,11–13,15–19]. Oral administration may be especially suitable for children and for patients with poor venous access [9,10,20]. More importantly,

Biomedical Optics Express, Vol. 4, No. 8 (August 2013): pg. 1305-1317. DOI.

side effects reported with oral administration of fluorescein have been fewer and milder [15,21], although isolated cases of anaphylactoid reactions have been reported [22,23].

The ability to image the retinal microvasculature longitudinally *in vivo* is important for improving our understanding of physiological and pathological processes. It may also allow earlier recognition of pathology at stages where successful intervention may be possible and facilitate comparison of response to different treatment modalities. Conventional FA provides a wide-field view of the retinal vasculature, but its transverse and axial resolution is severely limited by ocular monochromatic aberrations. Histological comparisons have shown that fundus FA incompletely depicts the capillary networks [24]. Adaptive optics ophthalmoscopy has improved significantly over the past decade, enabling extraordinary microscopic views of retinal structures. Using the adaptive optics scanning light ophthalmoscope (AOSLO), *in vivo* studies of normal and pathological retinal microstructure have explored the photoreceptor mosaic [25,26], retinal pigment epithelium [27,28], nerve fiber layer [29] and microvasculature. More recently, motion contrast processing techniques applied to AOSLO have improved the visualization of retinal capillaries and micro-angiopathic features [30–33]. A variety of image processing methods that create image contrast from blood flow have also been applied to image sets acquired using retinal functional imager [34–36], optical coherence tomography (OCT) [37–42] and adaptive optics OCT [43] to visualize the retinal vasculature. Furthermore, additional non-invasive techniques have been successfully applied to imaging the retinal microvasculature including entoptic view [44–46] and adaptive optics flood-illumination [47,48]. Studies to demonstrate the clinical utility of these techniques are ongoing [41].

Although the use of FA with the AOSLO has been demonstrated in primates [27,49] and rodents [50,51], it has not yet been explored in living human subjects. In this proof-of-concept manuscript, we report on the use of AOSLO FA for the *in vivo* visualization of normal human retinal microvasculature. We discuss imaging methodology, including instrument parameters, light safety, fluorescein dosage, fluorescein route of administration, and imaging window for sufficient fluorescence signal intensity.

Biomedical Optics Express, Vol. 4, No. 8 (August 2013): pg. 1305-1317. DOI.

2 - Methods

2.1 Human subjects

Ten subjects, 20 to 38 years of age (mean age 27, median age 25) with no significant past medical or ocular histories were recruited. Written informed consent was obtained after the nature and potential risks of the procedure were explained. This study adhered to the tenets of the Declaration of Helsinki and was approved by the Institutional Review Board of the New York Eye and Ear Infirmary.

2.2 Fluorescein

Fluorescein came in 5 mL sterile vials containing 100 mg/mL fluorescein (AK-FLUOR 10%, Akorn, Inc., Lake Forest, Illinois). Previous authors have described various methods to make oral intake more palatable, including mixing the fluorescein with sugar [21], using encapsulated fluorescein pills [11,12,14,15] and mixing fluorescein with citrus juice [10,13]. For our experiments, oral fluorescein was administered with 50 mL of orange juice to mask its taste. The subject was instructed to drink the mixture rapidly, and the time of consumption was recorded as time zero. An additional 50 mL of orange juice was provided to wash out the residual taste of the fluorescein. In cases where IV administration of fluorescein was necessary, administration was performed by a nurse.

For our experiments, the dose of fluorescein chosen was estimated to balance the risk of any adverse systemic effects of fluorescein with the estimated risk of retinal phototoxicity. For example, while a smaller dose of fluorescein reduces the risk of an adverse systemic reaction it produces a weaker fluorescence signal requiring more retinal exposure to the excitation light. Conversely, a larger dose of fluorescein carries a somewhat higher risk of adverse reaction but reduces the required exposure to light. With these requirements considered, a 20 mg fluorescein/kg body weight oral dose was chosen as the baseline fluorescein dose for all experiments. This dose is slightly lower than previously reported doses of 25 mg/kg or greater that gave adequate fluorescence intensity on FA [10,12,14,15].

Biomedical Optics Express, Vol. 4, No. 8 (August 2013): pg. 1305-1317. DOI.

From the ten subjects imaged, the first five subjects were used to gather preliminary data in optimizing the imaging protocol at 20 mg/kg oral fluorescein. As described in Table 1, our results present data on the next five subjects in a series of five experiments using one subject each. Experiments 2-4 were designed to evaluate comparisons between fluorescein dosage, fluorescein route of administration, and imaging modality, and thus required two separate imaging sessions. Given that the half-life of fluorescein sodium is 267 minutes [52], subjects from Experiments 2-4 were given a minimum five days' time between sessions to insure near total clearance of fluorescein from the body.

2.3 Imaging protocol

Axial length measurements were collected (IOL Master, Carl Zeiss Meditec AG, Jena, Germany) in order to calculate the AOSLO image scale in microns per pixel. Pixel size calculations were based on the Emsley schematic eye model [53]. Mydriasis and cycloplegia were induced with 1 drop each of 2.5% phenylephrine hydrochloride ophthalmic solution (Bausch&Lomb Inc., Tampa, FL) and 1% tropicamide ophthalmic solution (Akorn Inc., Lake Forest, IL). Color fundus photography (Topcon 3D OCT 2000, Topcon Corporation, Tokyo, Japan) was performed to provide clinical context to the retinal features seen with AOSLO imaging. Conventional scanning laser ophthalmoscope (SLO) FA (Heidelberg Spectralis HRA-OCT, Heidelberg Engineering Inc., Heidelberg, Germany) using oral fluorescein and FA (TRC 50IX Retinal Camera, Topcon Corporation, Tokyo, Japan) using IV fluorescein were performed for comparison with AOSLO FA (Table 1).

Stable and repeatable positioning of the subject's eye during AOSLO imaging was achieved using a bite bar attached to a translation stage that allowed for fine transverse and axial adjustments. A dental impression material was used to stabilize the subject's jaw on the bite bar (Splash! Putty, DenMat Holdings, LLC, Lompoc, California, USA). Transverse alignment of the subject was achieved by centering the pupil of the eye using the AOSLO wavefront sensor. Axial alignment was then achieved by maximizing the image intensity in the

Biomedical Optics Express, Vol. 4, No. 8 (August 2013): pg. 1305-1317. DOI.

reflectance channel and its uniformity across the field of view (FOV). Subjects were instructed to direct their gaze towards a green internal fixation target that was moved to allow imaging of specific locations of interest on the retina. During each imaging session, the reflectance channel was used to identify the regions of interest. Coordinates of these locations were recorded so that they could be re-imaged following fluorescein administration in the fluorescence channel. Optimal focus, determined for both the fluorescein excitation and reflectance channels, was recorded and used for all subsequent imaging of the identified locations.

Previous studies have reported that maximum excitation signal intensity occurs 15-60 minutes following oral administration of fluorescein with visibility of pathologic features present up to 120 minutes [9,11–15]. Given this information, AOSLO FA imaging sessions started at approximately 15 minutes post-administration of fluorescein in all experiments. In Experiments 3 and 4, AOSLO FA imaging began 15 minutes post-administration of fluorescein and continued at 20-minute intervals until 115 minutes had elapsed. During imaging, simultaneous segments of fluorescence and reflectance images consisting of 120-200 frames each were recorded at 15 frames per second using a 1°, 1.5° or 1.75° FOV. The gain of the detector in both channels was maintained at a constant level during all imaging sessions for all subjects. Throughout the imaging session, subjects were encouraged to blink frequently to support their normal tear film and were provided with short breaks of 3-5 minutes at regular intervals or as needed.

2.4 AOSLO

The AOSLO used for this study was a replica of the one by Dubra and Sulai [54], with the visible channel modified for fluorescence imaging. The modification involved replacement of the light source with a 488 nm diode laser (Lasos, Lasertechnick GmbH, Jena, Germany), and the addition of an interferometric band-pass optical filter centered at 525 nm with a 45 nm bandwidth in front of the detector. The longitudinal chromatic aberration (LCA) present in the human eye spreads the fluorescence focus along the optical axis over a range of approximately 0.3 diopters. This was addressed by

Biomedical Optics Express, Vol. 4, No. 8 (August 2013): pg. 1305-1317. DOI.

using a large (3.75 Airy disk diameter) confocal aperture. No attempt was made to account for LCA variation across individuals.

Both the reflectance and fluorescence registered averaged images with high signal-to-noise ratio were generated by applying the frame-to-frame estimated eye motion calculated from the reflectance images, using sequences of 40-100 raw frames [27,55]. Typically, it took an examiner one minute to select 4-5 reference frames from each video, and it took an additional minute for the software to create the registered image averages. The registered image averages were then tiled (Adobe Photoshop CS6, Adobe Systems, Inc., San Jose, California, USA) to create larger fields of view.

2.5 Light safety

During AOSLO FA, the retina was simultaneously exposed to up to three different light sources (488, 790 and 850 nm), which entered the eye as superimposed (coaxial), near-collimated 7.75 mm diameter beams. All three beams localized onto a single spot on the fundus, which was rapidly scanned to form a 1.3, 1.95 or 2.3° square imaging raster, using a 14.5 KHz horizontal resonant optical scanner and a 16 Hz vertical optical scanner. Synchronous modulation of the light sources turned them on at the start of the imaging portion of each horizontal line used for imaging when scanning from left to right. As a result only the central 1.0 to 1.75° of the scanning raster were exposed to light. The optical powers without modulation (i.e., continuous wave) measured at the cornea were 15 μW for the 850 nm wavefront sensing superluminescent diode (SLD), 100 μW for the 790 nm imaging SLD and 32 μW for the 488 nm diode laser. During imaging, the on/off modulation reduced the average powers delivered to approximately 25% of their original values.

No retinal location was exposed to the combined light sources for longer than 120 seconds. When immediately contiguous areas were imaged, the exposures were reduced to a maximum of 30 seconds to account for potential overlapping exposure of neighboring retinal locations due to involuntary eye motion. All sources were considered as lasers for the maximum permissible exposure (MPE) calculations, which were performed using the ANSI standard for the safe use of

Biomedical Optics Express, Vol. 4, No. 8 (August 2013): pg. 1305-1317. DOI.

lasers [56]. These imaging parameters, as described above, resulted in light exposures 6 times below both the photochemical and the thermal MPE limits.

3 - Results

In all 10 subjects, AOSLO FA was able to successfully resolve the smallest capillaries. Retinal vessels to the level of quaternary branches and capillary beds were clearly distinguishable from the rim of the optic disc to the foveal avascular zone (FAZ). Throughout the imaging session and during the six hours which followed, only one subject reported experiencing any adverse effects. The subject experienced transient nausea and heaving immediately following IV injection of fluorescein, which resolved shortly thereafter. As with conventional FA imaging, the intensity of the fluorescence in the AOSLO FA images varied over time, location and across individuals.

3.1 Experiment 1: comparison of AOSLO FA vs. conventional SLO FA using oral fluorescein

Images collected within 10 minutes of each other in a single subject using conventional scanning laser ophthalmoscope (SLO) FA and AOSLO FA, following oral administration of 20 mg/kg fluorescein, illustrate the superior resolution provided by the use of adaptive optics (Fig. 1). Numerous fine capillaries are revealed in the AOSLO FA images, which are not visible in the conventional SLO FA images.

3.2 Experiment 2: comparison of AOSLO FA using oral fluorescein vs. conventional IV FA

Conventional IV FA using a fundus camera was performed on a subject using 500 mg IV fluorescein. On a different visit, AOSLO FA images were collected, starting 15 minutes post-administration of oral (20 mg/kg) fluorescein. 1.75° FOV AOSLO images were collected contiguously to complete a 6° box centered at the fovea. Comparison of the AOSLO FA montage with conventional IV FA shows that AOSLO FA reveals much finer vasculature with appreciably higher contrast (Fig. 2).

Biomedical Optics Express, Vol. 4, No. 8 (August 2013): pg. 1305-1317. DOI.

3.3 Experiment 3: comparison of oral versus IV fluorescein in AOSLO FA

To assess the strength of the fluorescence signal as a function of time in oral versus IV administration, we imaged the same patient with AOSLO FA in two different imaging sessions. Oral fluorescein (20 mg/kg) was used in the first session, and IV fluorescein (500 mg) was used in the second session. AOSLO imaging began 15 minutes post-administration of fluorescein and continued at 20-minute intervals until 115 minutes had elapsed (Fig. 3). The mean pixel value of the resulting images was used as a metric for fluorescence signal. As shown in Fig. 3, oral and IV fluorescein provided similar image intensities at 17 minutes and 18 minutes after administration respectively. At 35 minutes or more after administration, oral fluorescein provided higher peak image intensity and more sustained fluorescence compared to IV fluorescein. It should be noted that peak intensity in the case of IV administration probably occurred before the first image of the sequence.

3.4 Experiment 4: AOSLO FA oral fluorescein dosimetry

In an effort to minimize potential adverse reactions to orally administered fluorescein, we explored the feasibility of visualizing retinal vasculature using a lower dose (7 mg/kg *vs*. 20 mg/kg). Figure 4 shows images from one area of interest that was imaged at both the high and low dose of fluorescein in two separate imaging sessions. As previously described, AOSLO imaging began 15 minutes post-administration of fluorescein and continued at 20-minute intervals until 115 minutes had elapsed. Similarly, the mean pixel value of the resulting images was used as a metric for fluorescence signal. The sequence of images shown in Fig. 4 demonstrate that comparable images were produced by both doses, although as expected, the fluorescence signal, as measured by the mean pixel values, scaled with the dose. Both doses, however, appear sufficient in most cases to allow for AOSLO FA imaging for as long as an hour, although this could vary significantly across visits and individuals.

Biomedical Optics Express, Vol. 4, No. 8 (August 2013): pg. 1305-1317. DOI.

3.5 Experiment 5: resolution of overlying peripapillary capillary beds using AOSLO FA

We examined the ability of AOSLO FA to axially resolve overlying capillary beds at 4 peripapillary locations (Fig. 5(A) insets B, C, D and E) using 20 mg/kg oral fluorescein. AOSLO FA was able to resolve the radial peripapillary capillary bed (Fig. 5(B2), 5(C2), 5(D2) and 5(E2)) within the highly reflective surface of the nerve fiber layer (Fig. 5(B1), (C1), (D1) and (E1)). As the focus shifted toward the outer retina, deeper capillary beds were resolved (Fig. 5(B3), 5(C3), 5(D3) and 5(E3)). Images of the deeper capillary beds appear somewhat noisier due to background haze from the out-of-focus fluorescence signal of the choroidal vasculature.

4 - Discussion

We have demonstrated that AOSLO FA can reveal microscopic detail of the retinal vasculature at safe light exposures in human subjects using oral or IV fluorescein. With both methods of fluorescein administration, AOSLO FA was able to visualize the retinal capillary beds at all attempted retinal locations and at multiple depths with qualitatively comparable contrast and sharpness. While both the 7 mg/kg oral dose and 500 mg IV dose successfully visualized the fine capillaries, the 20 mg/kg dose provided a stronger, more sustained fluorescence signal. Thus, 20 mg/kg oral administration of fluorescein seems more suitable for surveying larger retinal areas, given the current limited FOV (typically < 3°) of the AOSLO. It is important to note that, compared to conventional FA, the small FOV of the AOSLO limits its ability to acquire the early filling sequence of fluorescein over a large retinal area. Fluorescence peak and disappearance varied both across individuals and visits with both oral and IV fluorescein. Even with this variability, we were able to achieve up to an hour of sufficient signal intensity when using 20 mg/kg oral fluorescein.

Consistent with previous reports [15,21], adverse reactions to fluorescein occurred less frequently when administered orally. Only one adverse reaction (nausea and heaving) occurred following IV administration in this series, with none following oral administration. Since isolated case reports have described rare but occasionally severe

Biomedical Optics Express, Vol. 4, No. 8 (August 2013): pg. 1305-1317. DOI.

reactions to orally administered fluorescein, it is very important to elicit any patient history of atopy or past reactions to fluorescein [57]. Precautionary measures in the imaging laboratory such as ready access to a resuscitative crash cart are also recommended [5].

Currently, AOSLO FA appears to offer reasonable signal-to-noise ratio, no image processing artifacts, axial sectioning, and near-diffraction-limited transverse and axial resolution. For an average eye with effective focal length of approximately 17 mm and a pupil diameter of 7.75 mm, AOSLO FA approaches an axial resolving limit of 20 μm, enabling it to resolve overlying capillary beds in the retina [58]. However, a significant clinical limitation of AOSLO FA which must be considered is that the potential transverse and axial resolution of the AOSLO can only fully materialize with unobstructed large pupils. Lower reflectance and fluorescence signal and/or poorer resolution should be expected in subjects with small pupils and/or cataracts. AOSLO image quality can also be affected by non-clear media, retinal or anterior chamber inflammation and multifocal or diffractive intraocular lens implants. Imaging the vasculature with conventional (i.e., non-AO) OCT-based techniques, on the other hand, may be less affected by cataracts because they do not require a large pupil, although lower transverse resolution is to be expected. We believe that new and developing microvascular imaging technologies, including non-invasive motion contrast image processing techniques [34,35,37–39,43], will prove to be synergistic with AOSLO FA and perhaps better suited for fast non-invasive screening. Further studies are necessary to determine the full advantages and limitations of these emerging technologies relative to each other. AOSLO FA, although not likely to replace conventional wide-field FA, offers great potential for studying and quantifying retinal microvascular attributes such as vessel diameter, branching pattern, tortuosity and capillary density in both healthy and disease states. Much can be learned by applying already developed metrics and geometrical descriptors for retinal and brain vascular imaging [59–64]. Coupled with methods to quantify microvascular attributes, we believe that AOSLO FA will provide insights into retinal vascular diseases, and has the potential to become a clinical tool in detecting disease, disease progression, and tissue response to traditional and emerging treatment modalities. Furthermore, through studying and characterizing the retinal

Biomedical Optics Express, Vol. 4, No. 8 (August 2013): pg. 1305-1317. DOI.

microvascular changes that occur in systemic cardiovascular disease with AOSLO FA, we can potentially gain a deeper understanding of pathological processes and end-organ damage that occur in diabetes, hypertension and vascular occlusion [65,66].

Acknowledgments

The authors would like to thank Jennifer Hunter and Ethan Rossi for their assistance with the light safety calculations. Funding was provided by Marrus Family Foundation, Bendheim-Lowenstein Family Foundation, Wise Family Foundation, Chairman's Research Fund of the NYEEI, NIH grants R01EY017607, P30EY001931, UL1RR031973, an unrestricted departmental grant from Research to Prevent Blindness and the Glaucoma Research Foundation. A. Dubra is the recipient of a Career Development Award from Research to Prevent Blindness and a Career Award at the Scientific Interface from the Burroughs Wellcome Fund.

References and links

1. H. R. Novotny and D. L. Alvis, "A method of photographing fluorescence in circulating blood in the human retina," Circulation **24**(1), 82–86 (1961).

2. M. Abraham, J. T. Ahlman, A. J. Boudreau, and J. L. Connelly, *CPT 2011: Current Procedural Terminology* (American Medical Association Press, 2010).

3. L. A. Yannuzzi, *The Retinal Atlas, Har/Psc ED*. (Saunders, China, 2010).

4. D. C. Kalogeromitros, M. P. Makris, X. S. Aggelides, A. I. Mellios, F. C. Giannoula, K. A. Sideri, A. A. Rouvas, and P. G. Theodossiadis, "Allergy skin testing in predicting adverse reactions to fluorescein: a prospective clinical study," Acta Ophthalmol. (Copenh.) **89**(5), 480–483 (2011).

5. A. S. Kwan, C. Barry, I. L. McAllister, and I. Constable, "Fluorescein angiography and adverse drug reactions revisited: the Lions Eye experience," Clin. Experiment. Ophthalmol. **34**(1), 33–38 (2006).

6. L. A. Yannuzzi, K. T. Rohrer, L. J. Tindel, R. S. Sobel, M. A. Costanza, W. Shields, and E. Zang, "Fluorescein angiography complication survey," Ophthalmology **93**(5), 611–617 (1986).

7. F. J. Ascaso, M. T. Tiestos, J. Navales, F. Iturbe, A. Palomar, and J. I. Ayala, ""Fatal acute myocardial infarction after intravenous fluorescein angiography," Retina - J," Ret. Vit. Dis **13**, 238–239 (1993).

8. V. Fineschi, G. Monasterolo, R. Rosi, and E. Turillazzi, "Fatal anaphylactic shock during a fluorescein angiography," Forensic Sci. Int. **100**(1-2), 137–142 (1999).

9. J. S. Kelley and M. Kincaid, "Retinal fluorography using oral fluorescein," Arch. Ophthalmol. **97**(12), 2331–2332 (1979).

10. S. Ghose and B. K. Nayak, "Role of oral fluorescein in the diagnosis of early papilloedema in children," Br. J. Ophthalmol. **71**(12), 910–915 (1987).

11. F. M. Razvi, E. E. Kritzinger, M. D. Tsaloumas, and R. E. Ryder, "Use of oral fluorescein angiography in the diagnosis of macular oedema within a diabetic retinopathy screening programme," Diabet. Med. **18**(12), 1003–1006 (2001).

12. D. Squirrell, S. Dinakaran, S. Dhingra, C. Mody, C. Brand, and J. Talbot, "Oral fluorescein angiography with the scanning laser ophthalmoscope in diabetic retinopathy: a case controlled comparison with intravenous fluorescein angiography," Eye (Lond.) **19**(4), 411–417 (2005).

13. C. R. Garcia, M. E. Rivero, D. U. Bartsch, S. Ishiko, A. Takamiya, K. Fukui, H. Hirokawa, T. Clark, A. Yoshida, and W. R. Freeman, "Oral fluorescein angiography with the confocal scanning laser ophthalmoscope," Ophthalmology **106**(6), 1114–1118 (1999).

14. F. Gómez-Ulla, A. Malvar, M. Parafita, P. Polo, and I. Seoane, "Oral fluorescein angiography and fluoroscopy: determination of plasma fluorescein levels and clinical application," Optom. Vis. Sci. **69**(12), 986–990 (1992).

15. A. P. Watson and E. S. Rosen, "Oral fluorescein angiography: reassessment of its relative safety and evaluation of optimum conditions with use of capsules," Br. J. Ophthalmol. **74**(8), 458–461 (1990).

16. M. J. Noble, H. Cheng, and P. M. Jacobs, "Oral fluorescein and cystoid macular oedema: detection in aphakic and pseudophakic eyes," Br. J. Ophthalmol. **68**(4), 221–224 (1984).

17. R. Azad, B. K. Nayak, H. K. Tewari, and P. K. Khosla, "Oral fluorescein angiography," Indian J. Ophthalmol. **32**(5), 415–417 (1984).

18. R. V. Azad, B. Baishya, N. Pal, Y. R. Sharma, A. Kumar, and R. Vohra, "Comparative evaluation of oral fluorescein angiography using the confocal scanning laser ophthalmoscope and digital fundus camera with intravenous fluorescein angiography using the digital fundus camera," Clin. Experiment. Ophthalmol. **34**(5), 425–429 (2006).

19. R. Newsom, B. Moate, and T. Casswell, "Screening for diabetic retinopathy using digital colour photography and oral fluorescein angiography," Eye (Lond.) **14**(4), 579–582 (2000).

20. K. S. Morgan and R. M. Franklin, ""Oral fluorescein angioscopy in aphakic children," J Pediat. Ophth," Strab. **21**, 33–36 (1984).

21. T. Hara, M. Inami, and T. Hara, "Efficacy and safety of fluorescein angiography with orally administered sodium fluorescein," Am. J. Ophthalmol. **126**(4), 560–564 (1998).

22. F. P. Kinsella and D. J. Mooney, "Anaphylaxis following oral fluorescein angiography," Am. J. Ophthalmol. **106**(6), 745–746 (1988).

23. F. Gómez-Ulla, C. Gutiérrez, and I. Seoane, "Severe anaphylactic reaction to orally administered fluorescein," Am. J. Ophthalmol. **112**(1), 94 (1991).

24. K. R. Mendis, C. Balaratnasingam, P. Yu, C. J. Barry, I. L. McAllister, S. J. Cringle, and D. Y. Yu, "Correlation of histologic and clinical images to determine the diagnostic value of fluorescein angiography for studying retinal capillary detail," Invest. Ophthalmol. Vis. Sci. **51**(11), 5864–5869 (2010).

25. A. Roorda and D. R. Williams, "The arrangement of the three cone classes in the living human eye," Nature **397**(6719), 520–522 (1999).

26. J. Carroll, S. S. Choi, and D. R. Williams, "In vivo imaging of the photoreceptor mosaic of a rod monochromat," Vision Res. **48**(26), 2564–2568 (2008).

27. D. C. Gray, W. Merigan, J. I. Wolfing, B. P. Gee, J. Porter, A. Dubra, T. H. Twietmeyer, K. Ahamd, R. Tumbar, F. Reinholz, and D. R. Williams, "In vivo fluorescence imaging of primate retinal ganglion cells and retinal pigment epithelial cells," Opt. Express **14**(16), 7144–7158 (2006).

28. J. I. W. Morgan, A. Dubra, R. Wolfe, W. H. Merigan, and D. R. Williams, "In vivo autofluorescence imaging of the human and macaque retinal pigment epithelial cell mosaic," Invest. Ophthalmol. Vis. Sci. **50**(3), 1350–1359 (2008).

29. O. P. Kocaoglu, B. Cense, R. S. Jonnal, Q. Wang, S. Lee, W. Gao, and D. T. Miller, "Imaging retinal nerve fiber bundles using optical coherence tomography with adaptive optics," Vision Res. **51**(16), 1835–1844 (2011).

30. T. Y. Chui, D. A. Vannasdale, and S. A. Burns, "The use of forward scatter to improve retinal vascular imaging with an adaptive optics scanning laser ophthalmoscope," Biomed. Opt. Express **3**(10), 2537–2549 (2012).

31. T. Y. Chui, Z. Zhong, H. Song, and S. A. Burns, "Foveal avascular zone and its relationship to foveal pit shape," Optom. Vis. Sci. **89**(5), 602–610 (2012).

32. J. Tam, J. A. Martin, and A. Roorda, "Noninvasive visualization and analysis of parafoveal capillaries in humans," Invest. Ophthalmol. Vis. Sci. **51**(3), 1691–1698 (2010).

33. J. Tam, K. P. Dhamdhere, P. Tiruveedhula, S. Manzanera, S. Barez, M. A. Bearse, Jr., A. J. Adams, and A. Roorda, "Disruption of the retinal parafoveal capillary network in type 2 diabetes before the onset of diabetic retinopathy," Invest. Ophthalmol. Vis. Sci. **52**(12), 9257–9266 (2011).

34. Z. Burgansky-Eliash, A. Barak, H. Barash, D. A. Nelson, O. Pupko, A. Lowenstein, A. Grinvald, and A. Rubinstein, "Increased retinal blood flow velocity in patients with early diabetes mellitus," Retina **32**(1), 112–119 (2012).

35. Z. Burgansky-Eliash, D. A. Nelson, O. P. Bar-Tal, A. Lowenstein, A. Grinvald, and A. Barak, "Reduced retinal blood flow velocity in diabetic retinopathy," Retina **30**(5), 765–773 (2010).

36. D. A. Nelson, Z. Burgansky-Eliash, H. Barash, A. Loewenstein, A. Barak, E. Bartov, T. Rock, and A. Grinvald, "High-resolution wide-field imaging of perfused capillaries without the use of contrast agent," Clin Opthalmol **5**, 1095–1106 (2011).

37. V. J. Srinivasan, D. C. Adler, Y. Chen, I. Gorczynska, R. Huber, J. S. Duker, J. S. Schuman, and J. G. Fujimoto, "Ultrahigh-speed optical coherence tomography for three-dimensional and en face imaging of the retina and optic nerve head," Invest. Ophthalmol. Vis. Sci. **49**(11), 5103–5110 (2008).

38. T. Schmoll, A. S. G. Singh, C. Blatter, S. Schriefl, C. Ahlers, U. Schmidt-Erfurth, and R. A. Leitgeb, "Imaging of the parafoveal capillary network and its integrity analysis using fractal dimension," Biomed. Opt. Express **2**(5), 1159–1168 (2011).

39. Z. Zhi, X. Yin, S. Dziennis, T. Wietecha, K. L. Hudkins, C. E. Alpers, and R. K. Wang, "Optical microangiography of retina and choroid and measurement of total retinal blood flow in mice," Biomed. Opt. Express **3**(11), 2976–2986 (2012).

40. D. Y. Kim, J. Fingler, R. J. Zawadzki, S. S. Park, L. S. Morse, D. M. Schwartz, S. E. Fraser, and J. S. Werner, "Noninvasive imaging of the foveal avascular zone with high-speed, phase-variance optical coherence tomography," Invest. Ophthalmol. Vis. Sci. **53**(1), 85–92 (2012).

41. D. Y. Kim, J. Fingler, J. S. Werner, D. M. Schwartz, S. E. Fraser, and R. J. Zawadzki, "In vivo volumetric imaging of human retinal circulation with phase-variance optical coherence tomography," Biomed. Opt. Express **2**(6), 1504–1513 (2011).

42. S. Zotter, M. Pircher, T. Torzicky, M. Bonesi, E. Götzinger, R. A. Leitgeb, and C. K. Hitzenberger, "Visualization of microvasculature by dual-beam phase-resolved Doppler optical coherence tomography," Opt. Express **19**(2), 1217–1227 (2011).

43. Q. Wang, O. P. Kocaoglu, B. Cense, J. Bruestle, R. S. Jonnal, W. Gao, and D. T. Miller, "Imaging retinal capillaries using ultrahigh-resolution optical coherence tomography and adaptive optics," Invest. Ophthalmol. Vis. Sci. **52**(9), 6292–6299 (2011).

44. A. Bradley, H. Zhang, R. A. Applegate, L. N. Thibos, and A. E. Elsner, "Entoptic image quality of the retinal vasculature," Vision Res. **38**(17), 2685–2696 (1998).

45. M. Yap, J. Gilchrist, and J. Weatherill, "Psychophysical measurement of the foveal avascular zone," Ophthalmic Physiol. Opt. **7**(4), 405–410 (1987).

46. A. C. Bird and R. A. Weale, "On the retinal vasculature of the human fovea," Exp. Eye Res. **19**(5), 409–417 (1974).

47. J. Rha, R. S. Jonnal, K. E. Thorn, J. Qu, Y. Zhang, and D. T. Miller, "Adaptive optics flood-illumination camera for high speed retinal imaging," Opt. Express **14**(10), 4552–4569 (2006).

48. M. Lombardo, M. Parravano, S. Serrao, P. Ducoli, M. Stirpe, and G. Lombardo, "Analysis of Retinal Capillaries in Patients with Type 1 Diabetes and Nonproliferative Diabetic Retinopathy Using Adaptive Optics Imaging," Retina (to be published).

49. D. Scoles, D. C. Gray, J. J. Hunter, R. Wolfe, B. P. Gee, Y. Geng, B. D. Masella, R. T. Libby, S. Russell, D. R. Williams, and W. H. Merigan, "In-vivo imaging of retinal nerve fiber layer vasculature: imaging histology comparison," BMC Ophthalmol. **9**(1), 9 (2009).

50. D. P. Biss, D. Sumorok, S. A. Burns, R. H. Webb, Y. Zhou, T. G. Bifano, D. Côté, I. Veilleux, P. Zamiri, and C. P. Lin, "In vivo fluorescent imaging of the mouse retina using adaptive optics," Opt. Lett. **32**(6), 659–661 (2007).

51. D. P. Biss, R. H. Webb, Y. Zhou, T. G. Bifano, P. Zamiri, and C. P. Lin, "An adaptive optics biomicroscope for mouse retinal imaging," Proc. SPIE **6467**, 646703 (2007).

52. R. E. Barry and W. A. Behrendt, "Studies on the pharmacokinetics of fluorescein and its dilaurate ester under the conditions of the fluorescein dilaurate test," Arzneimittelforschung **35**(3), 644–648 (1985).

53. G. Smith and D. A. Atchison, *The Eye and Visual Optical Instruments,* 1st ed. (Cambridge University Press, Cambridge, 1997).

54. A. Dubra and Y. Sulai, "Reflective afocal broadband adaptive optics scanning ophthalmoscope," Biomed. Opt. Express **2**(6), 1757–1768

(2011).

55. A. Dubra and Z. Harvey, "Registration of 2D Images from Fast Scanning Ophthalmic Instruments " in *The 4th International Workshop on Biomedical Image Registration*, B. Fischer, B. M. Dawant, and C. Lorenz, ed. (Springer Berlin Heidelberg, Germany, 2010), pp. 60–71.

56. F. C. Delori, R. H. Webb, and D. H. Sliney, "Maximum permissible exposures for ocular safety (ANSI 2000), with emphasis on ophthalmic devices," J. Opt. Soc. Am. A **24**(5), 1250–1265 (2007).

57. E. Nucera, D. Schiavino, E. Merendino, A. Buonomo, C. Roncallo, E. Pollastrini, C. Lombardo, T. De Pasquale, and G. Patriarca, "Successful fluorescein desensitization," Allergy **58**(5), 458 (2003).

58. T. Wilson and A. R. Carlini, "Size of the detector in confocal imaging systems," Opt. Lett. **12**(4), 227–229 (1987).

59. M. K. Ikram, Y. T. Ong, C. Y. Cheung, and T. Y. Wong, "Retinal vascular caliber measurements: clinical significance, current knowledge and future perspectives," Ophthalmologica **229**(3), 125–136 (2013).

60. E. Zudaire, L. Gambardella, C. Kurcz, and S. Vermeren, "A computational tool for quantitative analysis of vascular networks," PLoS ONE **6**(11), e27385 (2011).

61. A. Perez-Rovira, T. MacGillivray, E. Trucco, K. S. Chin, K. Zutis, C. Lupascu, D. Tegolo, A. Giachetti, P. J. Wilson, A. Doney, and B. Dhillon, "VAMPIRE: Vessel assessment and measurement platform for images of the retina," in *Proceedings of IEEE Conference on Engineering in Medicine and Biology* Society (Institute of Electrical and Electronics Engineers, Boston, 2011), pp. 3391–3394.

62. M. B. Vickerman, P. A. Keith, T. L. McKay, D. J. Gedeon, M. Watanabe, M. Montano, G. Karunamuni, P. K. Kaiser, J. E. Sears, Q. Ebrahem, D. Ribita, A. G. Hylton, and P. Parsons-Wingerter, "VESGEN 2D: automated, user-interactive software for quantification and mapping of angiogenic and lymphangiogenic trees and networks," Anat. Rec. (Hoboken) **292**(3), 320–332 (2009).

63. G. Dougherty, M. J. Johnson, and M. D. Wiers, "Measurement of retinal vascular tortuosity and its application to retinal pathologies," Med. Biol. Eng. Comput. **48**(1), 87–95 (2010).

64. E. Bullitt, K. E. Muller, I. Jung, W. Lin, and S. Aylward, "Analyzing attributes of vessel populations," Med. Image Anal. **9**(1), 39–49 (2005).

65. J. Flammer, K. Konieczka, R. M. Bruno, A. Virdis, A. J. Flammer, and S. Taddei, "The eye and the heart," Eur. Heart J. **34**(17), 1270–1278 (2013).

66. T. Y. Wong and P. Mitchell, "Hypertensive retinopathy," N. Engl. J. Med. **351**(22), 2310–2317 (2004).

Table 1. AOSLO FA Experiments

Experiment	Session 1	Session 2
1	20 mg/kg oral; AOSLO FA & SLO FA	
2	20 mg/kg oral; AOSLO FA	500 mg IV; FA
3	20 mg/kg oral; AOSLO FA	500 mg IV; AOSLO FA
4	20 mg/kg oral; AOSLO FA	7 mg/kg oral; AOSLO FA
5	20 mg/kg oral; AOSLO FA & SLO FA	

Description of fluorescein dosages, routes of administration and imaging modalities used during imaging sessions in Experiments 1-5. Experiments 1 and 5 consisted of a single imaging session.

Biomedical Optics Express, Vol. 4, No. 8 (August 2013): pg. 1305-1317. DOI.

Fig. 1. Conventional SLO FA image (A) taken 20 minutes after oral administration of 20 mg/kg fluorescein, with two areas of interest (A insets B and C) approximately 5° from the fovea. These same areas were magnified and contrast stretched (B1 and C1) for comparison with AOSLO FA images of the corresponding areas (B2 and C2), collected 30 minutes after oral fluorescein administration. The scale bar represents 100 μm and applies to all images other than image A.

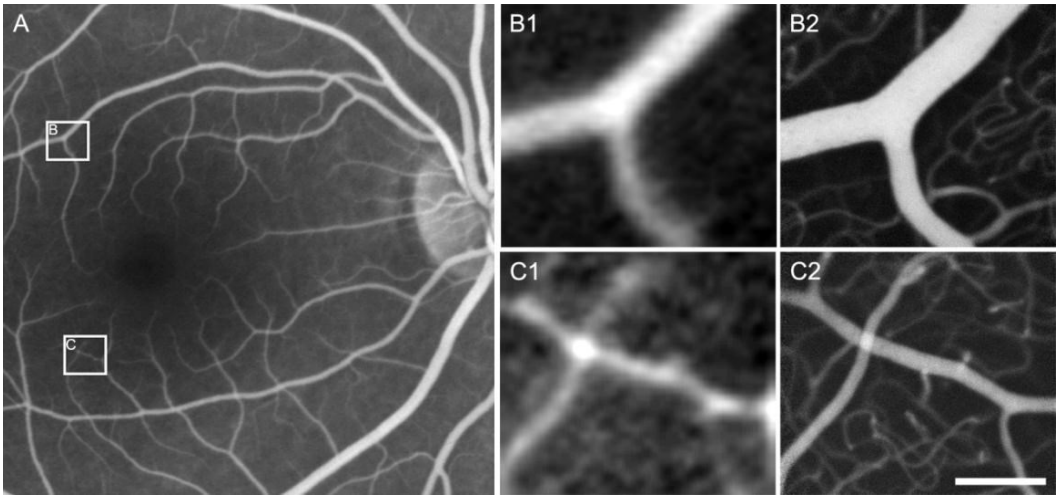

Biomedical Optics Express, Vol. 4, No. 8 (August 2013): pg. 1305-1317. DOI.

Fig. 2. Conventional IV FA image of the FAZ was magnified and contrast stretched (A) for comparison with an AOSLO FA image montage of the same region (B). The AOSLO scale bar represents 500 μm.

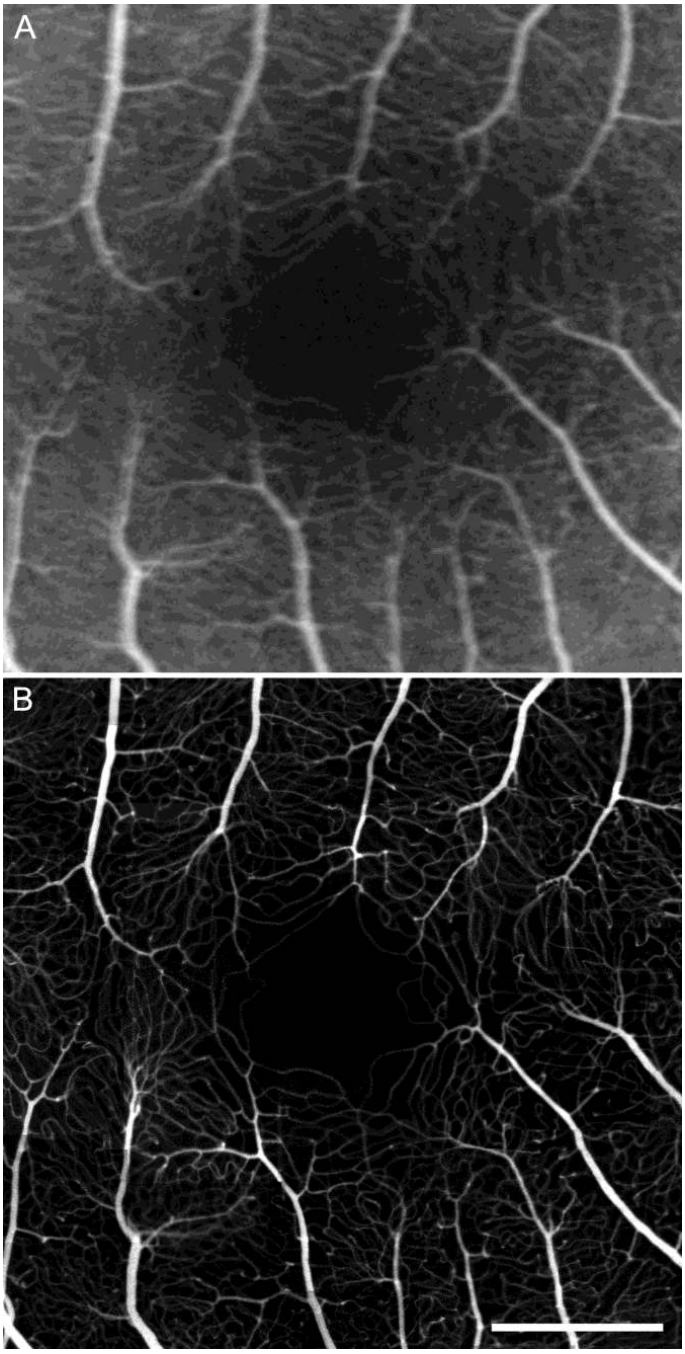

Biomedical Optics Express, Vol. 4, No. 8 (August 2013): pg. 1305-1317. DOI.

Fig. 3. Comparison of AOSLO FA image sequences after oral or IV fluorescein administration, showing a retinal area approximately 5° inferotemporal from the fovea. Fluorescein was administered at time zero. Mean pixel value was calculated for each image and then normalized to the maximum value of the oral and IV image series to generate the intensity percentages, presented on the top right corner of each image. All images were then contrast stretched to make optimal use of the gray scale while avoiding saturation. The contrast-stretched images are presented in this figure. The scale bar represents 100 μm.

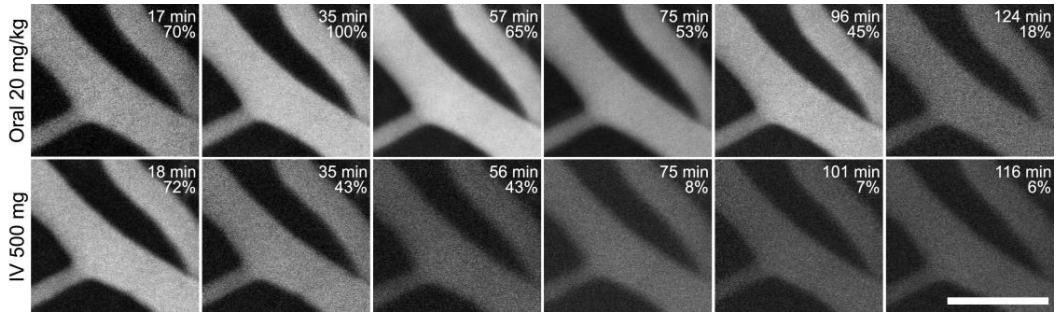

Fig. 4. Comparison of AOSLO FA image sequences between 20 mg/kg and 7 mg/kg oral administration of fluorescein, showing a retinal area approximately 5° superior-nasal from the fovea. Mean pixel values were calculated for each image and then normalized to the maximum value of the oral and IV image series to generate the intensity percentages, presented on the top right corner of each image. All images were then contrast stretched to make optimal use of the gray scale while avoiding saturation. The contrast-stretched images are presented in this figure. The scale bar represents 100 μm.

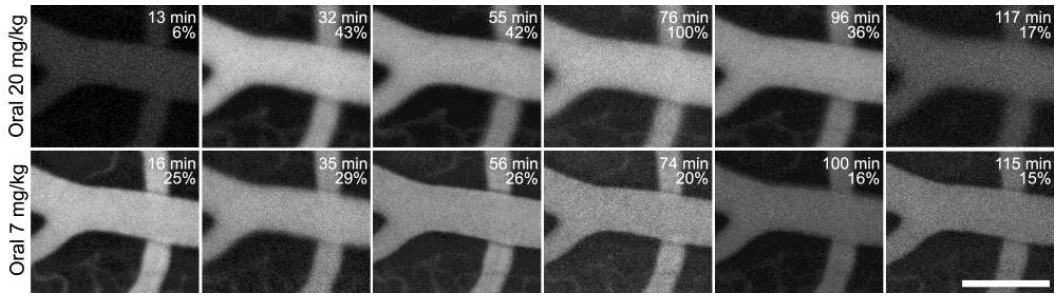

Biomedical Optics Express, Vol. 4, No. 8 (August 2013): pg. 1305-1317. DOI.

Fig. 5. Conventional SLO FA image acquired approximately 30 minutes after oral fluorescein administration (A) showing four peripapillary locations chosen for AOSLO imaging (A insets B, C, D and E). The reflectance AOSLO images of these small areas, focused on the nerve fiber layer (B1, C1, D1 and E1), show large blood vessels, capillaries and nerve fiber bundles. The corresponding AOSLO FA images recorded at the same focus (B2, C2, D2 and E2) approximately 15 minutes after oral fluorescein administration show only vasculature, revealing the radial peripapillary capillary bed with high contrast and detail. Peripapillary capillaries (B2, C2, D2 and E2) can be seen radiating parallel to the nerve fibers (B1, C1, D1 and E1). Capillary free zones can be seen surrounding arteries (B2, C2 and lower E2) and not veins (D2 and upper E2). AOSLO FA images focused closer to the outer retina (B3, C3, D3 and E3) show additional non-radial capillaries (arrow heads). These retinal capillaries can be seen deriving from the same retinal arteries (arrows) that supply the peripapillary capillaries. The scale bar represents 100 μm and applies to all images other than image A.

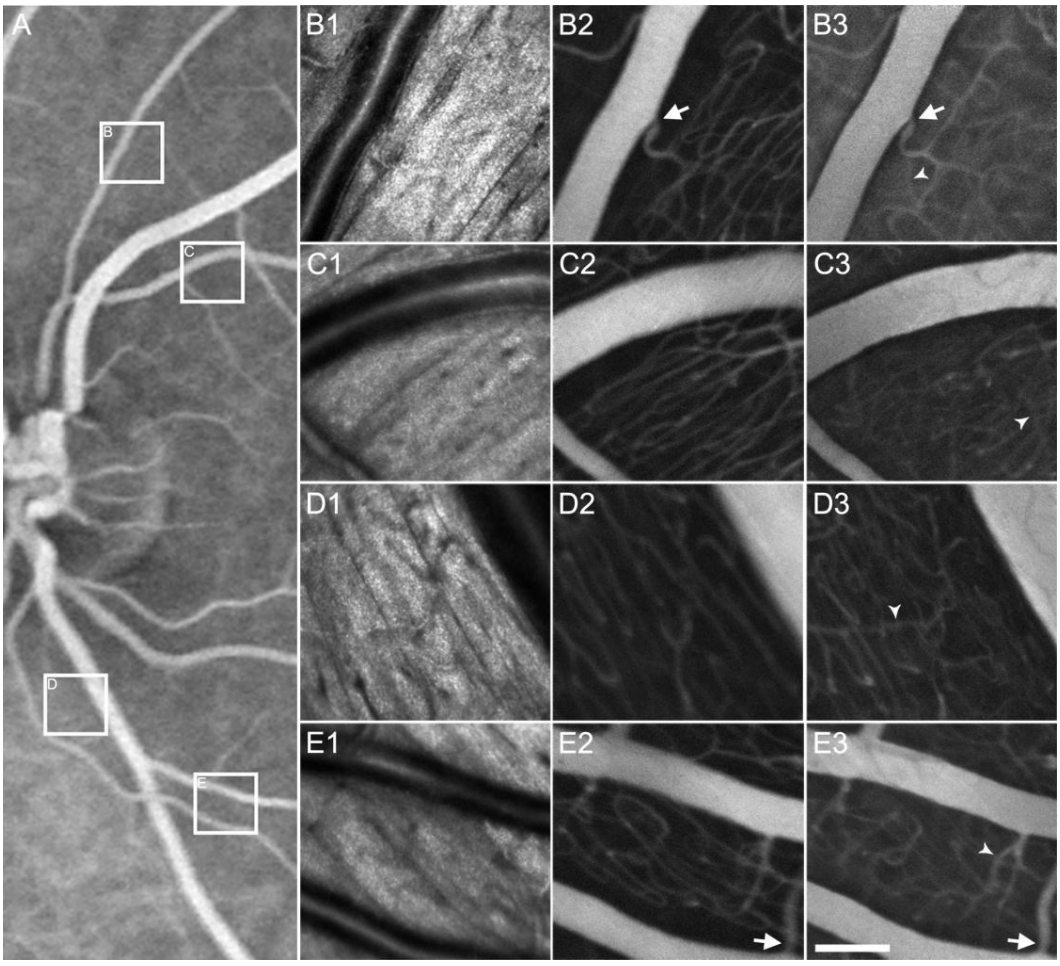

Biomedical Optics Express, Vol. 4, No. 8 (August 2013): pg. 1305-1317. DOI.